ACS APPLIED MATERIALS & INTERFACES

Research Article

www.acsami.org

Coating Solution for High-Voltage Cathode: AlF_3 Atomic Layer Deposition for Freestanding $LiCoO_2$ Electrodes with High Energy Density and Excellent Flexibility

Yun Zhou,[†] Younghee Lee,[‡] Huaxing Sun,[‡] Jasmine M. Wallas,[‡] Steven M. George,[‡] and Ming Xie*,[‡,§]

[†]College of Chemistry, Chongqing Normal University, Chongqing 401311, China

[‡]Department of Chemistry and Biochemistry, University of Colorado at Boulder, Boulder, Colorado 80309, United States

[§]BattFlex Technologies, Inc., Wuhan 430079, China

Supporting Information

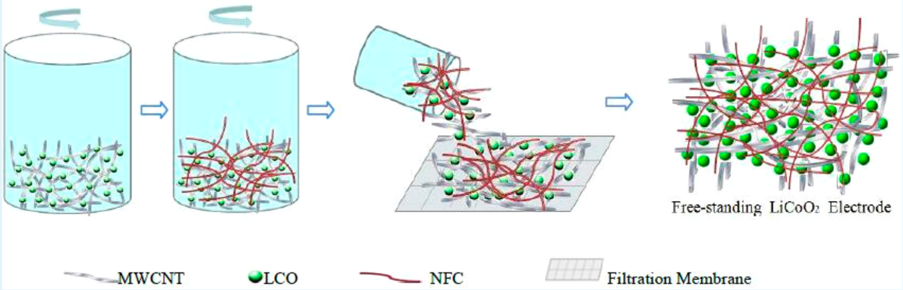

ABSTRACT: Freestanding $LiCoO_2$/multiwall carbon nanotube/nanocellulose fibril (LCO-MWCNT-NCF) electrodes are fabricated by a vacuum filtration technique. The electrode has a high LCO loading of 20 mg/cm^2 with excellent flexibility, uniform material distribution, and low surface resistivity. When coated with 2 ALD cycles of AlF_3, LCO-MWCNT-NCF has a high specific capacity of 216 mAh/g at 4.7 V. The freestanding AlF_3-coated electrode preserves 75.7% of its initial capacity after 100 cycles and 70% after 160 cycles of charge discharge. In contrast, electrodes coated with 2 ALD cycles of Al_2O_3 cannot be cycled above 4.5 V. By elimination of the unnecessary weight of current collector, and increasing in the working voltage simultaneously, this freestanding LCO-MWCNT-NCF electrode can significantly improve the gravimetric and volumetric energy density of lithium ion batteries.

KEYWORDS: *AlF_3, atomic layer deposition, freestanding, high energy density, excellent flexibility*

INTRODUCTION

The development of flexible electronic devices requires advanced lithium ion batteries (LIBs) with significant flexibility and high energy densities, including specific gravimetric and volumetric energy densities. There are two common routes to increase the energy density of a flexible LIB. The first method is to eliminate unnecessary weight, so-called "dead weight". The traditional electrode architecture contains active materials, conductive additives, polymeric binders, and current collectors, the last three of which do not contribute capacity to the battery. Significant efforts have been made to fabricate freestanding electrodes that do not require current collectors.[1−7] In our previous study, we successfully developed a freestanding electrode with an active material mass loading of 40 mg/cm^2 with only 8% carbon nanotube (CNT).[8] This electrode achieved a specific volumetric energy density of 400 mAh/cm^3, the highest reported value in the literature to date. However, CNTs are still very expensive. The CNT content of commercial cells is typically less than 2%. Therefore, there is an obvious demand to lower CNT content in freestanding electrodes in order to realize commercial feasibility.

The second common method used to increase energy density is to use high-capacity cathode materials stable at high voltages. Currently, $LiCoO_2$ (LCO) is the most widely used cathode material for consumer electronics due to its easy synthesis, high operating voltage, and high theoretical specific capacity. Recently, significant progress has been made to stabilize LCO at higher voltages, allowing more than 0.5 Li^+ to be extracted during the charging process.

Recently, atomic layer deposition (ALD) has been used as an advanced coating method for a variety of LIB electrodes.[9−12] ALD is a coating technique that relies on sequential, self-limiting surface reactions to grow conformal thin films, most typically oxides, with angstrom-level thickness control.[13] Some of the most striking LIB improvements with ALD have been achieved with Al_2O_3 coatings, demonstrating specific capacities up to 180 mAh/g when cycled to 4.5 V.[8,10,11] However, above 4.5 V LCO electrodes show significant performance degrada-

Received: December 7, 2016
Accepted: February 28, 2017
Published: February 28, 2017

© 2017 American Chemical Society

DOI: 10.1021/acsami.6b15628
ACS Appl. Mater. Interfaces 2017, 9, 9614−9619

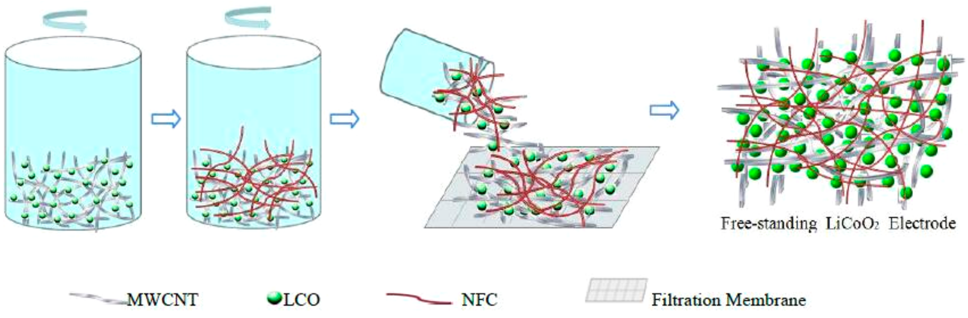

Figure 1. Schematic illustration of freestanding electrode preparation.

tion, indicating that Al_2O_3 is not suitable for voltages higher than 4.5 V. These metal oxide coatings are susceptible to attack by HF, a common LIB impurity, causing partial conversion of the coating to metal fluoride, producing H_2O, and effecting long-term cycling stability.[14−16] While ALD metal oxide coatings have contributed greatly to the enhancement of LIBs, the observed maximum voltage limit and the HF reactivity restrict the overall effectiveness of these coatings. Therefore, ALD coatings on electrodes that can enable higher voltage limits and do not exhibit reaction with HF are needed.

AlF_3 has shown promise as a protective electrode coating in LIBs.[17,18] Coatings of AlF_3, a wide band gap (>10 eV) material,[19,20] have been studied on both cathodes and anodes, demonstrating increased cycling stability.[17,18,21] Additionally, AlF_3 coatings may improve the thermal properties of cathodes by suppressing oxygen evolution at elevated temperatures.[22] Studies of AlF_3 ALD coatings on battery electrodes have been limited. Jackson et al. studied AlF_3 ALD deposited with TMA and TaF_5 as an electrode coating; however, their films had high impurity levels (>4%) and capacities well below those seen in Al_2O_3-ALD-coated electrodes.[23] J. S. Park et al.[24] reported aluminum−tungsten−fluoride (AlW_xF_y) films on LCO electrodes by ALD using TMA and tungsten hexafluoride (WF_6). Again, these ALD films did not exceed the performance of Al_2O_3 ALD coatings, with a maximum voltage of 4.4 V. Recently, Y. Lee et al.[25] reported a facile and low-impurity (<2%) AlF_3 ALD using trimethylaluminum (TMA) and HF from an HF−pyridine solution. This AlF_3 ALD coating is promising as an electrode protector, potentially allowing higher voltage ranges and higher energy densitites. To our knowledge, no other study has used this ALD method for battery coating studies.

In this work, we fabricated a freestanding LCO-MWCNT-NCF ($LiCoO_2$/multiwall carbon nanotube/nanocellulose fibrils) electrode with 2% of CNT and 5% of NCF. We then coated freestanding electrodes with AlF_3 ALD using the ALD system described by Y. Lee et al.[25] Several thicknesses of AlF_3 coatings were investigated to optimize LIB performance. The highest capacity observed in this study was 216 mAh/g at 4.7 V with a coating of 2 ALD cycles of AlF_3, corresponding to a volumetric density of 720 mAh/cm^3. After 100 cycles, the electrode still maintains 75.7% of its initial capacity after 100 cycles and 70% after 160 cycles at 4.7 V, indicating excellent cycling stability.

EXPERIMENTAL DETAILS

LCO was used as received from Sigma-Aldrich (99.8% trace metals basis). MWCNTs were purchased from NanoTechLabs Inc. with a large aspect ratio ∼10^4. NCF was purchased from NingBo ATMK Lithium Ion Technologies, Inc. It has a small diameter of ∼50 nm and a length up to 700 μm. AlF_3 and Al_2O_3 ALD films were grown on freestanding LCO-MWCNT-NCF electrodes using a hot wall ALD reactor employing static exposures of the reactants.

The AlF_3 ALD process using TMA and HF derived from HF−pyridine solution as precursors was employed for the AlF_3 coating on the electrode:[25]

$$AlF_3{-}HF^* + Al(CH_3)_3 \rightarrow AlF_3{-}AlF(CH_3)_2^* + CH_4 \tag{A}$$

$$AlF(CH_3)_2^* + HF \rightarrow AlF_3{-}HF^* + CH_4 \tag{B}$$

For the AlF_3 ALD, TMA (97%) and HF−pyridine (70 wt % HF) were obtained from Sigma-Aldrich.

The AlF_3 ALD reaction sequence follows: (i) dose TMA to 2.0 Torr; (ii) hold TMA pressure static for 30 s; (iii) evacuate reaction products and excess TMA for 60 s; (iv) flow 50 sccm N_2 for 360 s; (v) evacuate N_2 for 60 s; (vi) dose HF to 1.0 Torr; (vii) hold HF pressure static for 30 s; (viii) evacuate reaction products and excess HF for 60 s; (ix) flow 50 sccm N_2 for 360 s; (x) evacuate N_2 for 60 s. This sequence constitutes one cycle of AlF_3 ALD. This AlF_3 ALD was conducted at 150 °C.

An Al_2O_3 ALD process utilizing trimethylaluminum (TMA) and H_2O as precursors[26] was employed for Al_2O_3 coating on electrode.

$$AlOH^* + Al(CH_3)_3 \rightarrow AlO{-}Al(CH_3)_2^* + CH_4 \tag{C}$$

$$AlCH_3^* + H_2O \rightarrow AlOH + CH_4 \tag{D}$$

Al_2O_3 ALD used the same conditions except with H_2O instead of HF.

The electrodes were punched off from a 13 cm × 13 cm freestanding electrode, and then pressed to different thicknesses by a roll presser. All of the coin cells were assembled in an argon-filled glovebox with Li metal as the counter electrode. A Celgard separator 2340 and 1 M $LiPF_6$ electrolyte solution in 1:1 w/w ethylene carbonate/diethyl carbonate (Novolyte) were used. The galvanostatic charge/discharge characteristics were analyzed using an Arbin BT-2143 Battery Station.

RESULTS AND DISCUSSION

Freestanding electrodes were made using vacuum filtration with LCO particles as active material, 2% of MWCNTs as conductive additive, and 5% NCF as binder. A fabrication scheme is shown in Figure 1, and a more detailed description of the fabrication procedure can be found in previous publications.[2−5,8,27−29] The freestanding electrode used in this paper is 13 cm × 13 cm (Figure 2a), though vacuum filtration fabrication confers easy scale-up. The whole filtration time takes about 2 min. Without NCF, LCO with 2% MWCNT cannot be peeled off of the filtration membrane without mass loss due to the weak mechanical strength. When CNT content is increased to 8%, it is easy to peel off the electrode as a whole;[8] however, the cost is prohibitive. When 5% NCF is added with 2% CNTs, no residue is seen on the surface of the filtration membrane due to the strong hydrogen bond among nanocellulose fibers. This electrode is flexible enough to be

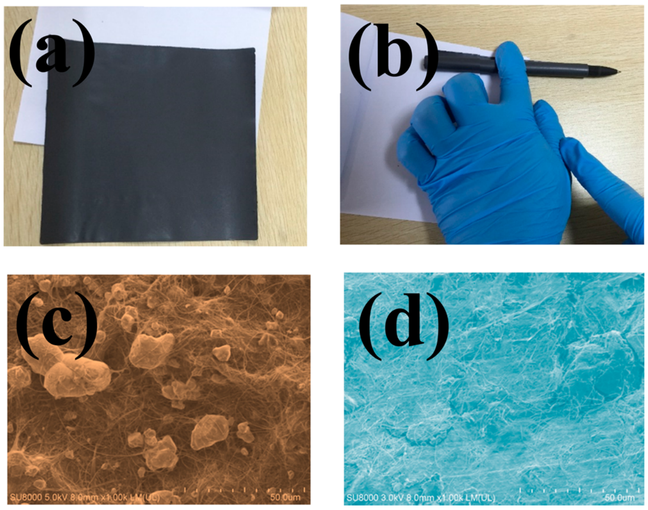

Figure 2. (a) A 13 cm by 13 cm freestanding paper electrode; (b) paper electrode that can be readily rolled; (c, d) SEM images of LCO uniformly embedded in a MWCNT matrix before and after compression.

easily rolled onto a pencil, as shown in Figure 2b. The scanning electron microscopy (SEM) images before and after compression (Figure 2c,d) show the uniform distribution of LCO particles in the continuous MWCNT and fibrillated nanocellulose network and the well-developed porous structure of the composite cathode. In Figure 2c, LCO particles are loosely tangled with MWCNTs and NCF, presenting an abundance of mesopores. After compression, the electrode thickness is greatly reduced from 220 to 60 μm, and LCO has much more contact with MWCNT and NCF. This corresponds to a compact density of 3.33 g/cm^3, slightly lower than that used in commercial products around 3.8−4.0 g/cm^3, but much higher than all of the freestanding electrodes previously published.[1−5,30] A low surface resistance of ∼5Ω/□ with only 8 wt % of MWCNTs is observed after compression, compared to ∼50 Ω/□ before compression. With 2% CNT and 5% NCF, the surface resistance reduces from 100 Ω/□ before compression to 30 Ω/□ after compression. This difference may deteriorate the electrode's C-rate capability. We also noticed that the thickness and surface resistance uniformity of freestanding electrodes are greatly improved to ±5% after compression.

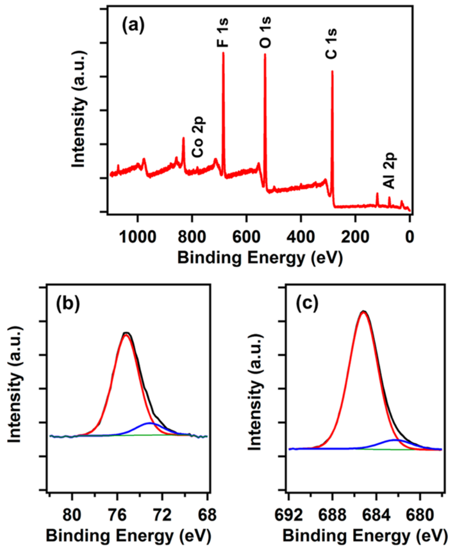

Figure 3. (a) XPS surface scan of an LCO-MWCNT electrode coated with 2 ALD cycles of AlF_3; (b) the XPS spectrum of the Al 2p peak; (c) the XPS spectrum of the F 1s peak.

AlF_3 ALD coatings on LCO-MWCNT electrodes were deposited in a hot wall reactor.[25] Al_2O_3 ALD coatings were also deposited in the same reactor. XPS analysis was performed to confirm the exsistence of the AlF_3 coating on the LCO-MWCNT electrodes. Figure 3a shows an XPS surface scan of an LCO-MWCNT electrode coated with 2 ALD cycles of AlF_3. XPS signals of C, O, F, Al, Co are observed with atomic percentages of 61.9, 24.4, 9.4, 4.1, and 0.3, respectively. The C peak arises from both carbon in the MWCNT and adventitious carbon. The Al and F peaks are assigned to the AlF_3 ALD coating. The Co peak is assigned to LCO. Figure 3b shows the XPS spectrum of the Al 2p peak located at 75.2 eV. The peak position consists of a main peak at 75.2 eV and a small peak at 73.2 eV. The Al 2p peak at the higher binding energy of 75.2 eV is in good agreement with the Al 2p peak at 74.80 eV obtained from an 82 nm AlF_3 film grown on Si with similar conditions. The additional Al 2p peak at a lower binding energy of 73.2 eV may be attributed to the Al−O bond resulting from the interaction between the AlF_3 film and moisture. Figure 3c shows the XPS spectrum of the F 1s peak at 685.2 eV. The F 1s peak at a higher binding energy of 685.2 eV is consistent with the F 1s peak at 685.2 eV observed in an 82 nm thick AlF_3 ALD film. The additional F 1s peak at a lower binding energy of 682.2 eV may be attributed to the Co−F or Li−F bonds resulting from the reaction of HF with LCO during the AlF_3 ALD film growth. These Al and F XPS signals from the AlF_3 coating increased due to the increased thickness of the AlF_3 coating.

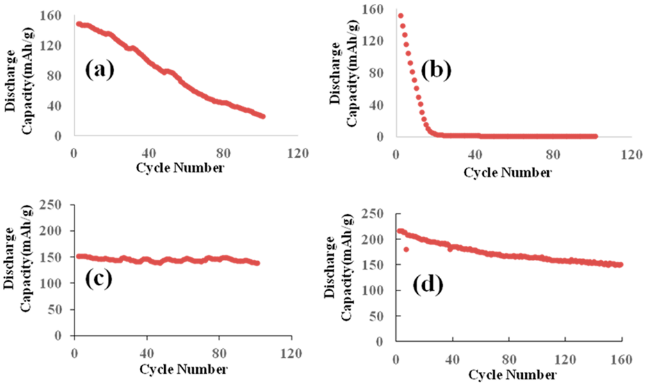

Figure 4. LCO-MWCNT coated with 2 cycles of Al_2O_3 is tested under 1 C rate at (a) 4.6 V and (b) 4.7 V; LCO-MWCNT coated with 2 cycles of AlF_3 is tested under 1 C rate at (c) 4.5 V and (d) 4.7 V. 1 C = 160 mA/g.

LCO-MWCNT-NCF coated with 2 cycles of Al_2O_3 is tested under 1 C rate at 4.6 and 4.7 V, respectively, in Figure 4. Figure 4a shows dramatic capacity loss of 82% of its initial capacity after 100 cycles at 4.6 V, and Figure 4b shows an even faster drop at 4.7 V. In our prevous work,[8] LCO-MWCNT-NCF with 2 cycles of Al_2O_3 still preserves 95% of its initial capacity after 85 cycles at 4.5 V. This indicates that the Al_2O_3 coating provides limited protection on LCO-MWCNT-NCF up to 4.5 V. Above 4.5 V, the Al_2O_3 coating either reacts severely with HF in the electrolyte or the organic electrolyte decomposes rapidly and forms a thick insulating film on the surface of LCO-MWCNT, preventing lithium ion diffusion.

In comparison to the Al_2O_3 coating, a coating of 2 cycles of AlF_3 on LCO-MWCNT-NCF shows a great improvement at 4.7 V. At 4.5 V, AlF_3 shows cycling performance stability comparable to that of Al_2O_3 in Figure 4c. When the upper voltage limit is increased to 4.7 V, AlF_3-coated LCO-MWCNT-NCF preserves 75.7% of its initial capacity after 100 cycles and 70% after 160 cycles at a rate of 0.5 C, as shown in Figure 4d. We would like to point out that the electrolyte used in this work is not designed for voltages above 4.5 V. The initial coulombic efficiency (CE) is 91.6%, and soon improves to above 99% after 5 cycles. In order to achieve 80% capacity retention after 400 cycles, CE should reach above 99.95%. Adding high-voltage additives should reduce electrolyte decomposition and further improve CE and cycling performance. The significant enhancement in capacity retention of AlF_3 at 4.7 V is likely due to increased HF resistance and stability at high voltage. AlF_3 has a lower Gibbs free energy than that of Al_2O_3,[31] which indicates intrinsically more stable nature. AlF_3 can also effectively suppress the fast growth of the solid electrolyte interphase film upon cycling.[32] The half-cell was disassembled after cycling, and no crack or electrode peeling was observed, indicating the excellent mechanical stability of the freestanding electrode. The surface of LCO after cycling is shown in SI Figure 1. No significant surface coating is observed compared to Figure 2d.

A flexible pouch cell was assembled with freestanding LCO-MWCNT-NCF as cathode and graphite/MWCNT-NCF as anode. The mass loadings of LCO and graphite were 20 and 10 mg/cm², respectively. Two pairs of electrodes were used. A video showing that the battery delivers a stable output voltage while bending can be found in SI.

The charge−discharge voltage profiles of AlF_3-ALD-coated LCO-MWCNT-NCF at 4.7 V are shown in Figure 5. The discharge curve of AlF_3-coated LCO-MWCNT displays a wide potential plateau near 3.9 V due to the coexistence of two pseudophases of a Li-dilute α-phase and a Li-concentrated β-phase.[33] LCO-MWCNT with 2 cycles of AlF_3 has a high specific capacity of 216 mAh/g at 4.7 V, and a corresponding volumetric energy density of 720 mAh/cm³. The gravimetric and volumetric energy densities of the freestanding electrodes are 18% and 21% higher, respectively, than an electrode with the same mass loading and a 16 μm Al current collector. That improvement can be even more profound for the anode due to the high density of Cu current collectors. By eliminating current collectors and increasing the charging voltage, one can significantly improve the energy density of batteries.

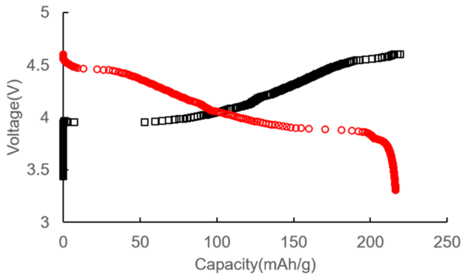

Figure 5. Charge−discharge voltage profile of LCO-MWCNT coated with 2 cycles of AlF_3 from 3.3 to 4.7 V. The current density is 0.5 C.

In order to study the optimum AlF_3 coating thickness, freestanding LCO-MWCNT-NCF electrodes coated with 2, 5, and 8 cycles of AlF_3 were tested under a 1 C rate shown in Figure 6. The voltage increases sequentially from 4.3 to 4.5, 4.6, and 4.7 V. In Figure 6a, LCO-MWCNT-NCF with 2 cycles of AlF_3 displays the highest capacity at all voltages, While LCO-MWCNT-NCF with 8 cycles of AlF_3 has the lowest, shown Figure 6c. Although the 5 cycle AlF_3-coated electrode has a limited capacity of 160 mAh/g at 4.7 V, it shows very stable cycling after 4.5 and 4.6 V for 10 cycles of charge/discharge. High-voltage stability of AlF_3 may be due to its larger band gap (10 eV for AlF_3 vs 6.2 eV for Al_2O_3).[19,20,34] As the thickness of the AlF_3 coating is increased, more energy is required to drive lithium ions across it. Therefore, we conclude that 2 cycles of AlF_3 strikes the balance between high-voltage protection and capacity realization.

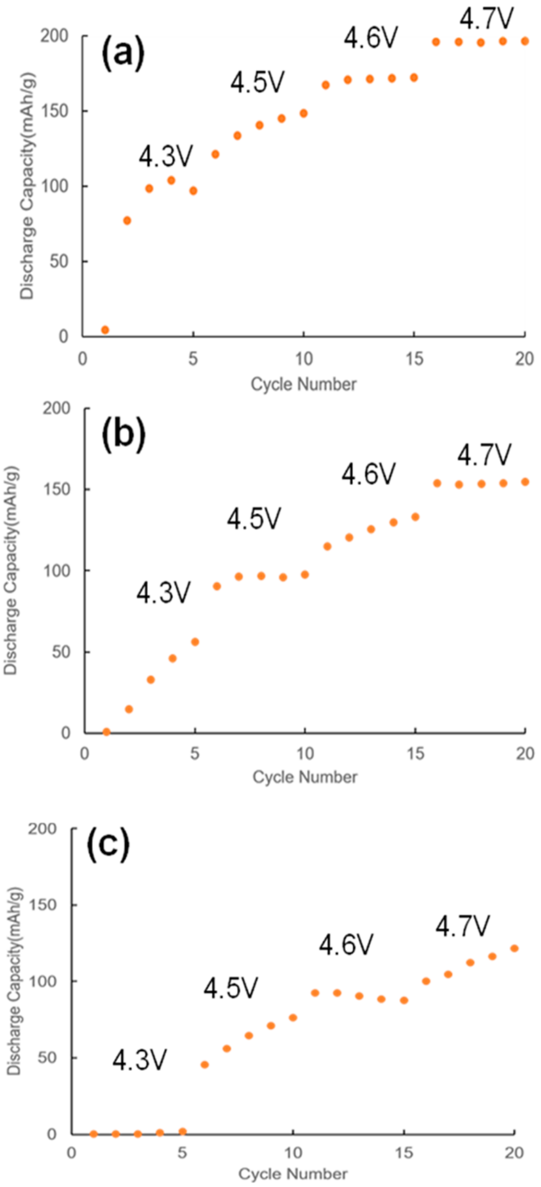

Figure 6. Freestanding LCO-MWCNT electrodes coated with (a) 2, (b) 5, and (c) 8 cycles of AlF_3 were tested under a 1 C rate. The voltage increases sequentially from 4.3 to 4.5, 4.6, and 4.7 V.

CONCLUSIONS

A 13 cm × 13 cm freestanding LCO-MWCNT-NCF paper electrode with high areal mass loading was fabricated by vacuum filtration. The electrode has a low CNT content of 2%, with 5% NCF, and a high LCO mass loading of 20 mg/cm^2. In addition, the electrode has excellent flexibility, uniform material distribution, and low surface resistivity. LCO particles are uniformly archored within a continuous three-dimensional conducting MWCNT and NCF matrix with significant mesoporous structure. After compression, LCO has better electrical contact with MWCNT and NCF and a reduced pore size. When coated with 2 cycles of Al_2O_3 by ALD, LCO-MWCNT-NCF cannot sustain cycling stability above 4.5 V and loses 82% of its initial capacity in the first 100 cycles at 4.6 V. When coated with 2 cycles of AlF_3 by ALD, LCO-MWCNT-NCF preserves 75.7% of its initial capacity after 100 cycles and 70% after 160 cycles at 4.7 V. This high capacity retention indicates that AlF_3 ALD coatings create exceptional high-voltage protection on cathodes, and deserve further exploration as battery coatings. The freestanding AlF_3-coated LCO-MWCNT-NCF electrode has a high capacity of 216 mAh/g at 4.7 V, and a correspondingly high volumetric energy density of 720 mAh/cm^3. With the combined effect of eliminating unnecessary weight and volume, and increasing charging voltage to offer more capacity, this freestanding electrode has an 18% higher gravimetric and 21% higher volumetric energy density than conventional electrodes with Al current collectors. To the best of our knowledge, our freestanding electrodes have the highest energy density in the literature, indicating great potential for flexible batteries with high energy density. Continuous production of a freestanding electrode is currently under study by BattFlex Technologies, Inc.

ASSOCIATED CONTENT

Supporting Information

The Supporting Information is available free of charge on the ACS Publications website at DOI: 10.1021/acsami.6b15628.

Images of relevant samples (PDF)

Video showing that the battery delivers a stable output voltage while bending (MP4)

AUTHOR INFORMATION

Corresponding Author

*E-mail: ming.xie@battflex.com.

ORCID

Yun Zhou: 0000-0003-3926-9405
Steven M. George: 0000-0003-0253-9184

Notes

The authors declare no competing financial interest.

ACKNOWLEDGMENTS

The work at Chongqing Normal University was supported by the Natural Science Foundation of China (21301199), Natural Science Foundation of Chongqing Municipality (cstc2014jcy-jA50035), and Chongqing Municipal Education Commission (KJ130601). Work at BattFlex Technologies Inc. was supported by the 3551 Recruitment Program of Global Experts by Wuhan East Lake Hi-Tech Development Zone, China. The work done at the University of Colorado, Boulder was supported by the Defense Advanced Research Project Agency (DARPA).

REFERENCES

(1) Hu, L.; La Mantia, F.; Wu, H.; Xie, X.; McDonough, J.; Pasta, M.; Cui, Y. Lithium-Ion Textile Batteries with Large Areal Mass Loading. *Adv. Energy Mater.* **2011**, *1* (6), 1012−1017.

(2) Fang, X.; Ge, M. Y.; Rong, J. P.; Zhou, C. W. Free-Standing LiNi0.5Mn1.5O4/Carbon Nanofiber Network Film as Lightweight and High-Power Cathode for Lithium Ion Batteries. *ACS Nano* **2014**, *8* (5), 4876−4882.

(3) Choi, K.-H.; Cho, S.-J.; Chun, S.-J.; Yoo, J. T.; Lee, C. K.; Kim, W.; Wu, Q.; Park, S.-B.; Choi, D.-H.; Lee, S.-Y.; Lee, S.-Y. Heterolayered, One-Dimensional Nanobuilding Block Mat Batteries. *Nano Lett.* **2014**, *14* (10), 5677−5686.

(4) Ban, C. M.; Li, Z.; Wu, Z. C.; Kirkham, M. J.; Chen, L.; Jung, Y. S.; Payzant, E. A.; Yan, Y. F.; Whittingham, M. S.; Dillon, A. C. Extremely Durable High-Rate Capability of a LiNi0.4Mn0.4Co0.2O2 Cathode Enabled with Single-Walled Carbon Nanotubes. *Adv. Energy Mater.* **2011**, *1* (1), 58−62.

(5) Luo, S.; Wang, K.; Wang, J. P.; Jiang, K. L.; Li, Q. Q.; Fan, S. S. Binder-Free LiCoO2/Carbon Nanotube Cathodes for High-Performance Lithium Ion Batteries. *Adv. Mater.* **2012**, *24* (17), 2294−2298.

(6) Deng, X.; Xie, K.; Li, L.; Zhou, W.; Sunarso, J.; Shao, Z. Scalable synthesis of self-standing sulfur-doped flexible graphene films as recyclable anode materials for low-cost sodium-ion batteries. *Carbon* **2016**, *107*, 67−73.

(7) Chu, S.; Zhong, Y.; Cai, R.; Zhang, Z.; Wei, S.; Shao, Z. Mesoporous and Nanostructured TiO2 layer with Ultra-High Loading on Nitrogen-Doped Carbon Foams as Flexible and Free-Standing Electrodes for Lithium-Ion Batteries. *Small* **2016**, *12* (48), 6724−6734.

(8) Xie, M.; Li, B.; Zhou, Y. Free-standing high-voltage LiCoO2/multi-wall carbon nanotube paper electrodes with extremely high areal mass loading for lithium ion batteries. *J. Mater. Chem. A* **2015**, *3* (46), 23180−23184.

(9) Guan, D.; Jeevarajan, J. A.; Wang, Y. Enhanced cycleability of LiMn2O4 cathodes by atomic layer deposition of nanosized-thin Al2O3 coatings. *Nanoscale* **2011**, *3* (4), 1465−1469.

(10) Jung, Y. S.; Cavanagh, A. S.; Dillon, A. C.; Groner, M. D.; George, S. M.; Lee, S.-H. Enhanced Stability of LiCoO2 Cathodes in Lithium-Ion Batteries Using Surface Modification by Atomic Layer Deposition. *J. Electrochem. Soc.* **2010**, *157* (1), A75−A81.

(11) Scott, I. D.; Jung, Y. S.; Cavanagh, A. S.; Yan, Y.; Dillon, A. C.; George, S. M.; Lee, S.-H. Ultrathin Coatings on Nano-LiCoO2 for Li-Ion Vehicular Applications. *Nano Lett.* **2011**, *11* (2), 414−418.

(12) Zhao, J.; Wang, Y. Ultrathin Surface Coatings for Improved Electrochemical Performance of Lithium Ion Battery Electrodes at Elevated Temperature. *J. Phys. Chem. C* **2012**, *116* (22), 11867−11876.

(13) George, S. M. Atomic Layer Deposition: An Overview. *Chem. Rev.* **2010**, *110* (1), 111−131.

(14) Sun, Y.-K.; Cho, S.-W.; Lee, S.-W.; Yoon, C. S.; Amine, K. AlF3-Coating to Improve High Voltage Cycling Performance of Li [Ni1/3Co1/3Mn1/3]O2 Cathode Materials for Lithium Secondary Batteries. *J. Electrochem. Soc.* **2007**, *154* (3), A168−A172.

(15) Myung, S.-T.; Izumi, K.; Komaba, S.; Sun, Y.-K.; Yashiro, H.; Kumagai, N. Role of Alumina Coating on Li−Ni−Co−Mn−O Particles as Positive Electrode Material for Lithium-Ion Batteries. *Chem. Mater.* **2005**, *17* (14), 3695−3704.

(16) Kim, J. W.; Kim, D. H.; Oh, D. Y.; Lee, H.; Kim, J. H.; Lee, J. H.; Jung, Y. S. Surface chemistry of LiNi0.5Mn1.5O4 particles coated by Al2O3 using atomic layer deposition for lithium-ion batteries. *J. Power Sources* **2015**, *274*, 1254−1262.

(17) Sun, Y. K.; Lee, M. J.; Yoon, C. S.; Hassoun, J.; Amine, K.; Scrosati, B. The Role of AlF_3 Coatings in Improving Electrochemical Cycling of Li-Enriched Nickel-Manganese Oxide Electrodes for Li-Ion Batteries. *Adv. Mater.* **2012**, *24* (9), 1192−1196.

(18) Ding, F.; Xu, W.; Choi, D. W.; Wang, W.; Li, X. L.; Engelhard, M. H.; Chen, X. L.; Yang, Z. G.; Zhang, J. G. Enhanced Performance of Graphite Anode Materials by AlF_3 Coating for Lithium-Ion Batteries. *J. Mater. Chem.* **2012**, *22* (25), 12745−12751.

(19) Barriere, A. S.; Lachter, A. Optical-Transitions in Disordered Thin-Films of Ionic Compounds MgF_2 and AlF_3 as a Function of Their Conditions of Preparation. *Appl. Opt.* **1977**, *16* (11), 2865−2871.

(20) Konig, D.; Scholz, R.; Zahn, D. R. T.; Ebest, G. Band Diagram of the $AlF_3/SiO_2/Si$ System. *J. Appl. Phys.* **2005**, *97* (9), 093707.

(21) Zheng, J. M.; Zhang, Z. R.; Wu, X. B.; Dong, Z. X.; Zhu, Z.; Yang, Y. The Effects of AlF_3 Coating on the Performance of $Li[Li_{0.2}Mn_{0.54}Ni_{0.13}Co_{0.13}]O_2$ Positive Electrode Material for Lithium-Ion Battery. *J. Electrochem. Soc.* **2008**, *155* (10), A775−A782.

(22) Myung, S. T.; Lee, K. S.; Yoon, C. S.; Sun, Y. K.; Amine, K.; Yashiro, H. Effect of AlF_3 Coating on Thermal Behavior of Chemically Delithiated $Li_{0.35}[Ni_{1/3}Co_{1/3}Mn_{1/3}]O_2$. *J. Phys. Chem. C* **2010**, *114* (10), 4710−4718.

(23) Jackson, D. H. K.; Laskar, M. R.; Fang, S.; Xu, S.; Ellis, R. G.; Li, X.; Dreibelbis, M.; Babcock, S. E.; Mahanthappa, M. K.; Morgan, D.; Hamers, R. J.; Kuech, T. F. Optimizing AlF3 atomic layer deposition using trimethylaluminum and TaF5: Application to high voltage Li-ion battery cathodes. *J. Vac. Sci. Technol., A* **2016**, *34* (3), 031503.

(24) Park, J. S.; Mane, A. U.; Elam, J. W.; Croy, J. R. Amorphous Metal Fluoride Passivation Coatings Prepared by Atomic Layer Deposition on LiCoO2 for Li-Ion Batteries. *Chem. Mater.* **2015**, *27* (6), 1917−1920.

(25) Lee, Y.; DuMont, J. W.; Cavanagh, A. S.; George, S. M. Atomic Layer Deposition of AlF3 Using Trimethylaluminum and Hydrogen Fluoride. *J. Phys. Chem. C* **2015**, *119* (25), 14185−14194.

(26) Dillon, A. C.; Ott, A. W.; Way, J. D.; George, S. M. Surface chemistry of Al2O3 deposition using Al(CH3)3 and H2O in a binary reaction sequence. *Surf. Sci.* **1995**, *322* (1−3), 230−242.

(27) Jabbour, L.; Bongiovanni, R.; Chaussy, D.; Gerbaldi, C.; Beneventi, D. Cellulose-based Li-ion batteries: a review. *Cellulose* **2013**, *20* (4), 1523−1545.

(28) Jabbour, L.; Destro, M.; Chaussy, D.; Gerbaldi, C.; Penazzi, N.; Bodoardo, S.; Beneventi, D. Flexible cellulose/LiFePO4 paper-cathodes: toward eco-friendly all-paper Li-ion batteries. *Cellulose* **2013**, *20* (1), 571−582.

(29) Lu, H.; Behm, M.; Leijonmarck, S.; Lindbergh, G.; Cornell, A. Flexible Paper Electrodes for Li-Ion Batteries Using Low Amount of TEMPO-Oxidized Cellulose Nanofibrils as Binder. *ACS Appl. Mater. Interfaces* **2016**, *8* (28), 18097−18106.

(30) Wu, Z. Z.; Han, X. G.; Zheng, J. X.; Wei, Y.; Qiao, R. M.; Shen, F.; Dai, J. Q.; Hu, L. B.; Xu, K.; Lin, Y.; Yang, W. L.; Pan, F. Depolarized and Fully Active Cathode Based on Li-(Ni0.5Co0.2Mn0.3)O-2 Embedded in Carbon Nanotube Network for Advanced Batteries. *Nano Lett.* **2014**, *14* (8), 4700−4706.

(31) Sun, Y.-K.; Lee, M.-J.; Yoon, C. S.; Hassoun, J.; Amine, K.; Scrosati, B. The Role of AlF3 Coatings in Improving Electrochemical Cycling of Li-Enriched Nickel-Manganese Oxide Electrodes for Li-Ion Batteries. *Adv. Mater.* **2012**, *24* (9), 1192−1196.

(32) Sun, S. W.; Yin, Y. F.; Wan, N.; Wu, Q.; Zhang, X. P.; Pan, D.; Bai, Y.; Lu, X. AlF3 Surface-Coated Li[Li0.2Ni0.17Co0.07Mn0.56]O-2 Nanoparticles with Superior Electrochemical Performance for Lithium-Ion Batteries. *ChemSusChem* **2015**, *8* (15), 2544−2550.

(33) Choi, Y.-M.; Pyun, S.-I.; Bae, J.-S.; Moon, S.-I. Effects of lithium content on the electrochemical lithium intercalation reaction into LiNiO2 and LiCoO2 electrodes. *J. Power Sources* **1995**, *56* (1), 25−30.

(34) Afanas'ev, V. V.; Houssa, M.; Stesmans, A.; Heyns, M. M. Band alignments in metal−oxide−silicon structures with atomic-layer deposited Al2O3 and ZrO2. *J. Appl. Phys.* **2002**, *91* (5), 3079−3084.